ISTITUTO NAZIONALE DI FISICA NUCLEARE

Sezione di Milano

INFN/AE-83/7
24 Ottobre 1983

P. G. Rancoita: SILICON DETECTORS AND ELEMENTARY PARTICLE PHYSICS

Servizio Documentazione
dei Laboratori Nazionali di Frascati

Istituto Nazionale di Fisica Nucleare
Sezione di Milano

INFN/AE-83/7
24 Ottobre 1983

P. G. Rancoita(x): SILICON DETECTORS AND ELEMENTARY PARTICLE PHYSICS

Invited talk given at the "Conference on Nuclear Structure and Elementary Particle Physics", Liverpool, 22-25 March, 1983;
to appear in Journal of Physics G.

ABSTRACT

Silicon detectors are currently a major instrument in high-energy physics experiments. The analysis of their energy-loss data (whose deviation from the Landau-Vavilov theories has been recently studied) is performed to determine the decay point of short-lived DD particles. To use them in colliding beam machine experiments technological developments have been undertaken in order to achieve a large scale integration for readout chips. They can find application in calorimetry as dense active sampling layer. The silicon sandwich calorimeters are well-suited to operate near the vacuum pipes.

1. - INTRODUCTION

Technological advances enabled to build very thin and large size area silicon detectors and fast associated electronics. At present the silicon counters are a major instrument in high-energy physics (for a review on the subject see ref. (1)).

The development of thin strip electrodes, the so-called microstrip dectector, yield a resolution of $\approx 5\ \mu m$[2]. The new microstrip devices, associated or not with multilayer silicon target, are intended to be employed in experiments of incoherent hadro- or photo-production of charmed and beauty particles, since this physics requi

---

(x) - CEN, Saclay (France), on leave from INFN-Milano (Italy).

res high-resolution tracking devices in order to detect vertics which are closer to the interaction point.

Further increase of the active area of silicon detectors together with LSI, Large Scale Integration (ref. (3) and see sect. 4), chips makes them attractive as inner vertex detectors in colliding beam machine experiments.

The use of low-resistivity inexpensive silicon detectors is investigated in order to replace scintillation counters in calorimetry[4], especially in magnetic environment or where there are geometric constraints or in vacuum pipe.

This paper presents a survey of the detector features and applications in high-energy physics experiments. The trend of the development is discussed by considering the use of these detectors in the forthcoming colliding beam machine experiments.

Section 2 deals with the general characteristics of silicon devices, their associated electronics, data processing for multilayer target and the modified energy-loss distribution.

In section 3 the charge-sharing between strips, the efficiency and the magnetic field effect in microstrip detectors are considered.

A survey of experiments at fixed target and colliding beam machines is presented in section 4.

2. - GENERAL CHARACTERISTICS

2. 1. - Silicon detectors and associated electronics

Silicon is the predominant semiconductor material used in production of radiation detectors.

Detection of nuclear radiation is based on the process of ionization or excitation of atoms in the detection medium by the passage of a charged particle (see sect. 2. 2). The number of electron-hole (e-h) pairs produced by a relativistic particle is ≈ 80 e-h/μm.

Silicon detectors can be made very thin. The typical thickness used in high-energy physics varies between 100 and 500 μm. So far the employed devices are both surface-barrier and ion-implanted detectors. Their resistivity is between 2 and 10 kΩ cm. The bulk silicon is usually n-type.

Surface-barrier detectors are made at room temperature. The usual treatment is the etching of the surface, then an evaporated metal, usually gold, is employed as the rectifying contact and aluminium as the ohmic one.

Another method of creating junctions is to expose a silicon crystal to a beam of ions produced by an accelerator. This method is called ion implantation and can be used to form n^+ or p^+ layers by accelerating either phosphorus or boron ions respectively. The concentration of impurity at the surface or at the most probable penetration depth (X_p) can be varied either by the ion bombardment energy or by the angle of incidence during the implantation process. However the impurity concentration extends its tail up to $5X_p$.

Compared with surface barriers, ion implanted detectors are more stable and less subject to ambient conditions.

A new method of manufacturing silicon detectors[5] based on a process (planar) which combines oxide passivation with ion implantation has been developed.

A great deal of development has provided hybrid and monolitic preamplifiers at low price and (together with their associated receivers or amplifiers) fast response. In Table I a simplified subdivision of electronic characteristics is presented as function of the input capacitance to the preamplifier (the very large input capacitance refers to calorimetric application).

TABLE I - Characteristics of electronics.

Input capacitance (pf)	FWHM (noise) (keV)	Base-time of signal
< 20	20	40 ns
<200	30	65 ns
<3000	150	1 μs

Recently, studies on radiation damage effects induced by relativistic particles have been carried out. The ion-implanted detectors show degraded operations (i. e. a strong increse of the leakage current) for a fluence greater than that required by surface-barrier devices[6]. In general the lower the resistivity the better the detector performance. A more specific investigation found that full depletion and full charge collection can be obtained by increasing the reverse bias voltage[7]. This way normal operations were obtained up to fluence value of 8.3×10^{13} relativistic protons cm^{-2}.

2. 2. - Multilayer silicon data and modified energy-loss distribution

The energy-loss data, namely the energy released in the detector, is recorded when the Si-counters are the target and are arranged as a multilayer telescope, along the beam direction (see sect. 4). A maximum likelihood analysis is usually performed

in order to define the number of particles traversing each detector. This way the position of the decay vertex of the short-lived particle is reconstructed.

Let us now consider the simplest situation, namely a coherent reaction with only one short-lived particle decay inside the device (this method can be easily generalized to two decay vertices and incoherent reactions). To fit the decay position, X, one has to assume that n relativistic particles are leaving the production detector and that, from position X, m particles are present. Furthermore we suppose that X is located in between the layer j and j+1. The likelihood function $L(X,n,m)$[1] is just the product of the differential probabilities of obtaining the energy-loss actually measured, assuming that the decay occurred at position X and we have:

$$L(X,n,m) = \Pi_{i=1,j} \Lambda(\Delta_i, n)\, \Pi_{i=j+1,f} \Lambda(\Delta_i, m) \qquad (1)$$

where $\Lambda(\Delta_i, p)$ is the probability density of getting the actually measured energy-loss Δ_i in the ith detector, assuming p relativistic particles crossing it; f is the total number of detectors and 1 is the 1st device after the production detector. Once the likelihood function is defined we have to consider its logarithmic function $l(X,n,m)$

$$l(X,n,m) = -2 \ln L(X,n,m) \qquad (2)$$

which has the significance of a χ^2 function[1].

The best estimate for X (the position of the decay point), n (the number of particles produced in the interaction) and m (the number of particles after the decay) is given by X, n, m for which l is minimum.

In order to evaluate correctly the likelihood function $L(X,n,m)$ a precise knowledge of the energy-loss distribution is required.

The silicon detectors commonly employed have to be considered thin absorbers, whereas the statistical nature of the ionization process on the passage of a fast charged particle results in strong fluctuations of the energy-loss.

The energy straggling function, $f_{L,V}(x, \Delta)$, is the solution of the transport equation:

$$\partial f_{L,V}(x, \Delta)/\partial x = \left(\int_0^b \omega'(\varepsilon') f_{V,L}(x, \Delta - \varepsilon')\, d\varepsilon' - f_{L,V}(x, \Delta) \int_0^{Em} \omega'(\varepsilon)\, d\varepsilon\right) x^{-1} \qquad (3)$$

where $\omega'(\varepsilon) = (\xi/\varepsilon^2)\left[1 - \beta^2(\varepsilon/Em)\right]$ is the Rutherford cross-section on free electron, Em is the maximum transferable energy in a collision, $\xi = 153.4(z^2/\beta^2)(Z/A)xp$ keV = $= 5.35/\beta^2$ keV for a charged particle traversing 300 μm of silicon, z and βc are the charge and the velocity of the incoming particle, ε is the transferred energy in a collision, x is the thickness of the absorber in cm.

Landau[8] solved eq. (3) by using a Laplace transform method and assuming b = = Em = ∞. The Landau distribution is given by

$$f_L(x, \Delta) = (1/\xi)\Phi(\lambda)$$

where $\Phi(\lambda) = (1/2\pi i)\int_{r-i\infty}^{r+i\infty} \exp(u\ln(u) + \lambda u)du$, r is an arbitrary real positive constant. The function $\Phi(\lambda)$ is a universal function of the dimensionless variable λ:

$$\lambda = (1/\xi)(\Delta - \langle\Delta\rangle) - \beta^2 - \ln(\xi/Em) - 1 + C = (1/\xi)\left[\Delta - (\Delta_{mp} - \xi\lambda_o)\right]$$

where C is the Euler constant 0.577215, λ_o is the value for which Φ is a maximum, Δ_{mp} is the most probable energy-loss for the Landau distribution. The function $\Phi(\lambda)$ has been tabulated by Boersch-Supan[9]. The full-width-at-half-maximum (FWHM) of the Landau distribution is $\approx 4\xi$. The ξ parameter has the meaning of an energy scale parameter.

In the Vavilov[10] solution of eq. (3), the proper maximum transferable energy has been taken into account, i. e. $b = \Delta$ for $\Delta < Em$ and $b = Em$ for $\Delta > Em$. However for $k = \xi/Em \to 0$, $f_V(x, \Delta) \to f_L(x, \Delta)$. For all practical purposes this limit is already satisfied for protons with kinetic energy greater than 150-200 MeV, traversing 300 μm of silicon absorber[11, 12]. In the following, only the Landau function will be considered.

The modified energy-loss distribution takes into account the effect of distant collisions, namely interactions in which the binding electron energy cannot be neglected. The energy straggling function is given by refs. (13, 14) (see also appendix of ref. (1)):

$$f(\Delta, x) = 1/(\sigma\sqrt{2\pi})\int_{-\infty}^{+\infty} f_L(\Delta, x)\exp\left[-(\Delta - \varepsilon)^2/2\sigma^2\right]d\varepsilon \qquad (4)$$

where Δ is the actual energy-loss when a thickness x of material is traversed.

The standard deviation of the convolving gaussian is

$$\sigma^2 = \delta_2 = M_2 - M_2'$$

where M_2 and M_2' are the second order moment of the modified cross-section taking into account the effect of electron binding and the Rutherford cross-section respectively.

Bichsel[15] has shown that further higher moments give negligible contributions.

The value of σ can be computed following Shulek et al.[16]

$$\sigma^2 = (8/3)\xi\Sigma_i l_i(Z_i/Z)\ln(2m_e c^2\beta^2/l_i) \qquad (5)$$

where l_i is the ionization potential of the ith shell[17], Z_i is the number of electrons in the ith shell of the stopping material and the summation is carried out over those shells for which $l_i < 2m_e c^2 \beta^2$. In the prediction of Bichsel and Yu[18,19], the σ^2 value increases as ln for $\beta \rightarrow 1$:

$$\sigma^2 = 2\xi\left[C_1 + C_2(2\ln(\beta\gamma) - \beta^2)\right]$$

where $C_1 \rightarrow 6$ keV and $C_2 \rightarrow 0.29$ keV in silicon for $\beta \rightarrow 1$.

The energy-loss sensed by a detector is described by eq. (4), whereas the convolving Gaussian has the standard deviation σ_t given by :

$$\sigma_t^2 = \sigma^2 + \sigma_{noise}^2$$

σ_{noise} is the standard deviation of the gaussian noise distribution.

If n relativistic particles are traversing a detector, we expect that the energy--loss distribution is :

$$\Lambda(\Delta, n) = f(\Delta, nx) \qquad (6)$$

where $\xi_n = n\xi$, $\sigma_t^2 = n\sigma^2 + \sigma_{noise}^2$, and $\Delta_{n,mp} = n(\Delta_{mp} + \xi \ln(n))$.

The values of Δ_{mp}, dE/dx (average stopping power) and σ for charged hadrons (π, k, p) have been investigated in the kinetic energy range between 0.25 GeV and 115 GeV[12,20].

In Fig. 1, the values of dE/dx and Δ_{mp} are given for $\beta\gamma$ in the range 1.1-336. As expected no relativistic rise is observed. The agreement with the Bethe-Block formula is satisfactory, when both the restriction[21] and the density effect are taken into account.

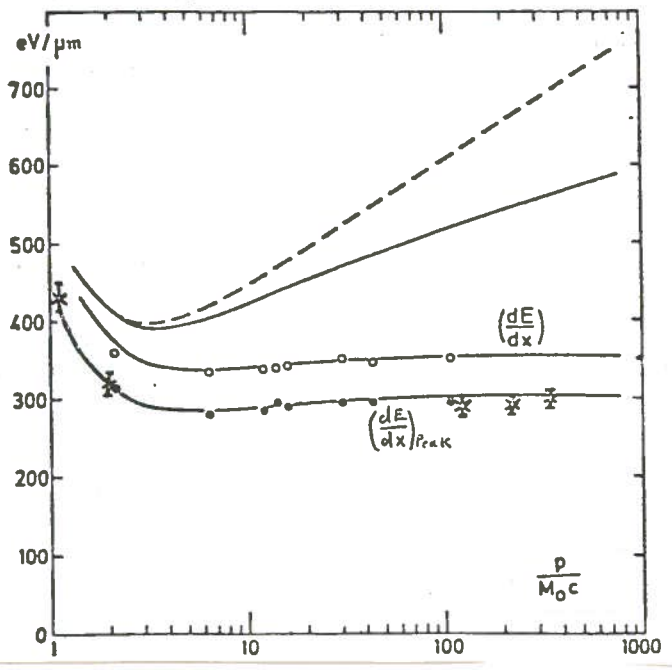

FIG. 1 - Energy-loss in silicon (in eV/μm) versus the parameter $P/M_o c = \beta\gamma$. The data (•) and (o) are for a 900 μm thick detector[20]. The data (⁎) are for a 300 μm thick detector[12]. The curves are from top: average stopping power without (dashed curve) and with (full curve) density effect. Average stopping power with both restriction[21] and density effect taken into account. The prediction of the most probable energy-loss compared to the experimental points.

The measured σ values (Fig. 2 from ref. (12)) are in agreement with the Shulek et al. predictions (eq. (5)).

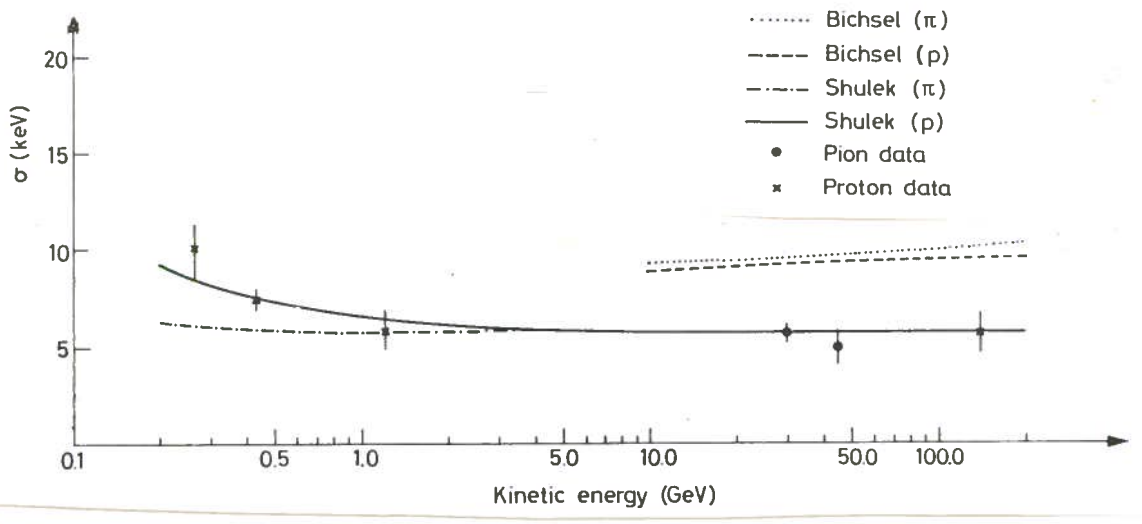

FIG. 2 - Measured values of the parameter σ [12]. The continuous and the dashed and dotted lines are the predictions of Shulek et al. for proton and pion respectively. The dashed and the dotted lines are the predictions of Bichsel[18], for proton and pion respectively.

In Fig. 3 two energy-loss spectra are shown[12]. The curves are the fitted functions, namely the modified energy-loss distribution given by eq. (4). The standard deviation of the noise contribution was measured before the data taking. Its value was $\approx 4.0 \pm 0.4$ keV.

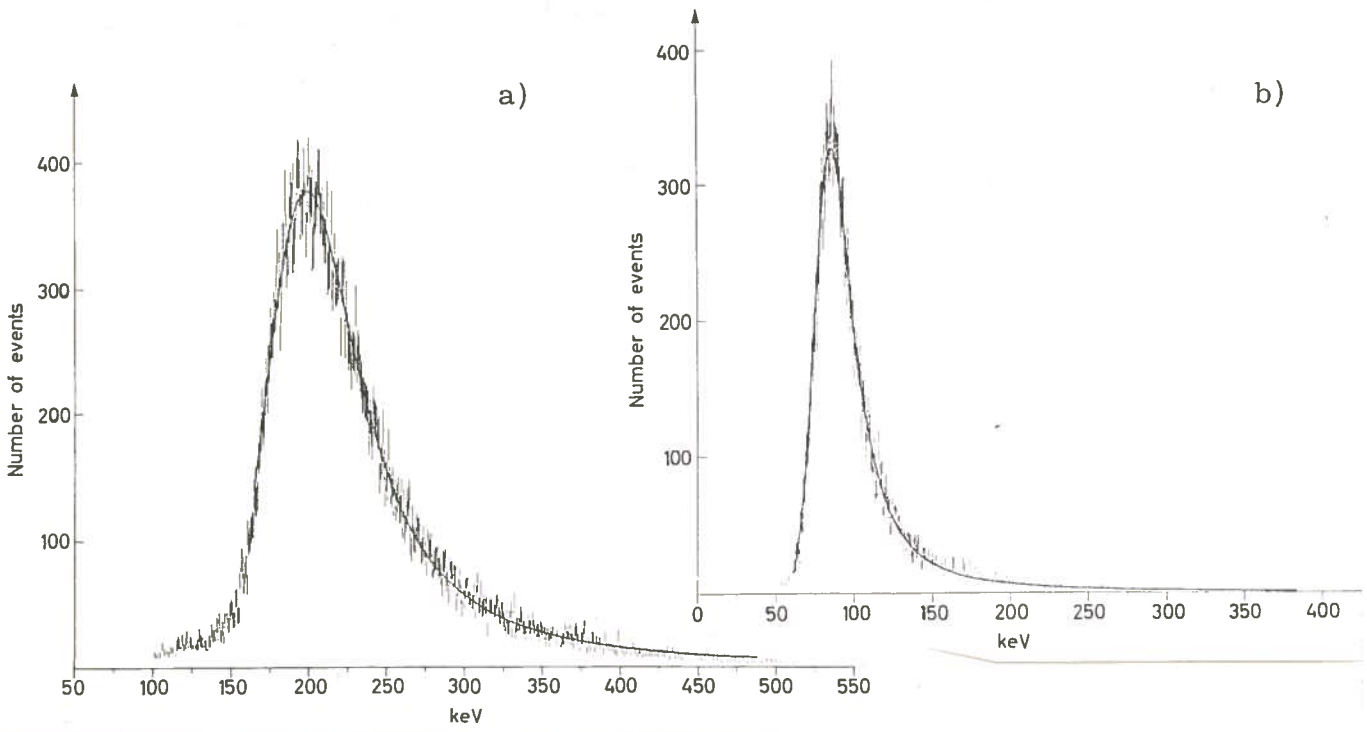

FIG. 3 - Figs. a) and b) show the energy-loss spectra at 0.736 and 115 GeV/c of incoming proton momenta respectively. The continuous curves are the complete fits to the experimental data. The values of ξ are 15.0 ± 0.8 and 5.6 ± 0.3 respectively. The values of σ are 10.2 ± 1.4 and 5.7 ± 1.1 respectively.

A study of the energy-loss of several relativistic particles has been performed at CERN-SPS[22]. The incoming proton beam had a momentum of 115 GeV/c. The final multiplicities were selected in a forward acceptance cone of 2.3^{o}, by employing of a microstrip detector. In Fig. 4 a multiparticle spectrum is shown.

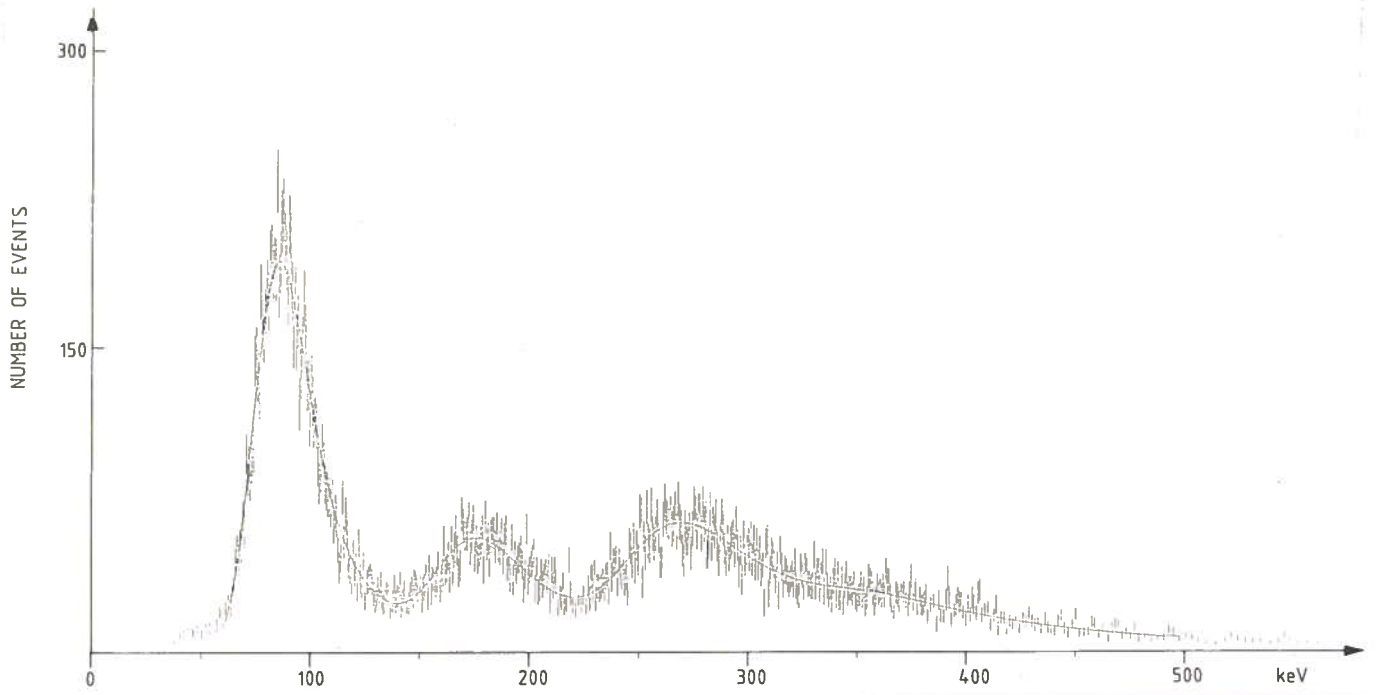

FIG. 4 - Energy-loss spectra including both single and several relativistic particles. The percentages, P(n), of the number of particles produced are: 0.41, 0.19, 0.31, 0.09 for one, two, three and four particles respectively. The continuous lines are the fitted curves.

The single particle (beam particle) constitutes about 41% of the events. The full line is the fitted curve, in which the free parameters are the values of σ and ξ for the single particle and the relative contents of one, two, three and four particles. In the fitting procedure, the energy-loss distribution of n particles is given by eq. (6). There is a good agreement between the experimental spectrum and the fitted curve.

3. - MICROSTRIP DEVICES

A microstrip detector is a silicon device in which the junction side or the rear side is made by strip electrodes. The strip pitch is the distance between the middle of two adjacent interstrips (see Fig. 5). Microstrip detectors can be currently made with strip pitch of $20\,\mu$m and strip length of 6 cm.

3.1. - Charge-sharing and efficiency

The charge-sharing (between neighbouring strips) and the efficiency have been investigated for both surface-barrier and ion-implanted silicon detectors[23] at CERN-

-PS. The momentum of the incoming pion beam was 10 GeV/c.

The beam particle traversing a surface-barrier detector generated both single and double hit events[24] (the triple hit events were negligible). In Fig. 6 (from ref. (23), the overall energy-loss (including both single and double hit events) is shown for a 400 μm thick detector. The charge-sharing effect characteristic of double hits is responsable of the event accumulation for energies lower than the most probable. In facts, the data sample selected requiring single hit events shows an energy-loss distribution (Fig. 7a), which is well represented by eq. (4). The percentage of double hits could be related to the interstrip resistance. However it cannot be easily controlled during the manufacturing process.

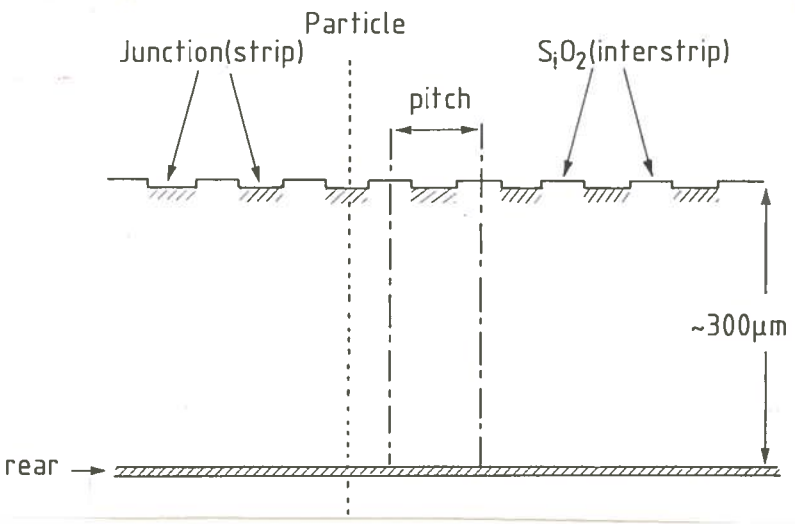

FIG. 5 - Section view of a microstrip detector.

The ion-implanted detector did not show any particular double hit phenomenon. In Fig. 7b, the overall energy-loss distribution sensed by a strip is given. It is well represented by eq. (4). At present the commonly employed microstrip detectors are ion-implanted.

Both the ion-implanted and surface-barrier devices had an efficiency compatible with 100%[23].

3. 2. -Capacitive charge sharing device

The capacitive charge division detector has been developed[2] in order to reduce the number of readout channels. In the device, i) the intermediate strips are kept at the same potential of the readout strips, ii) the impedance between readout strips is much greater than the input impedance of the electronics in order to avoid cross-talk, iii) the interstrip capacitance is greater than the strip-to-ground capacitance. In this way, the charge collected at intermediate strips can be divided amongst the neighbouring readout strips. The impact position of the incoming particle is found by computing the centre of gravity of the collected charge. The signals from the associated electronics have a base-time of about 800 ns.

The detectors made for the NA11 experiment at CERN-SPS have 20 μm pitch strips and a readout channel every three strips. In this way a spatial resolution of about 5 μm and two particle separation of 120 μm can be obtained.

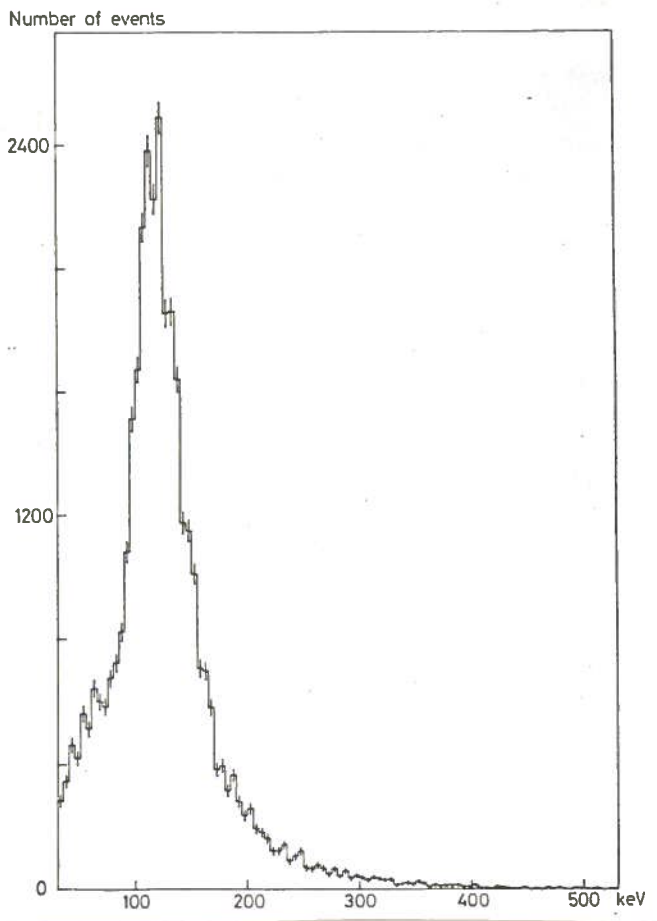

FIG. 6 - Total energy-loss distribution as sensed by a 400 μm thick and 200 μm strip pitch surface-barrier detector[23].

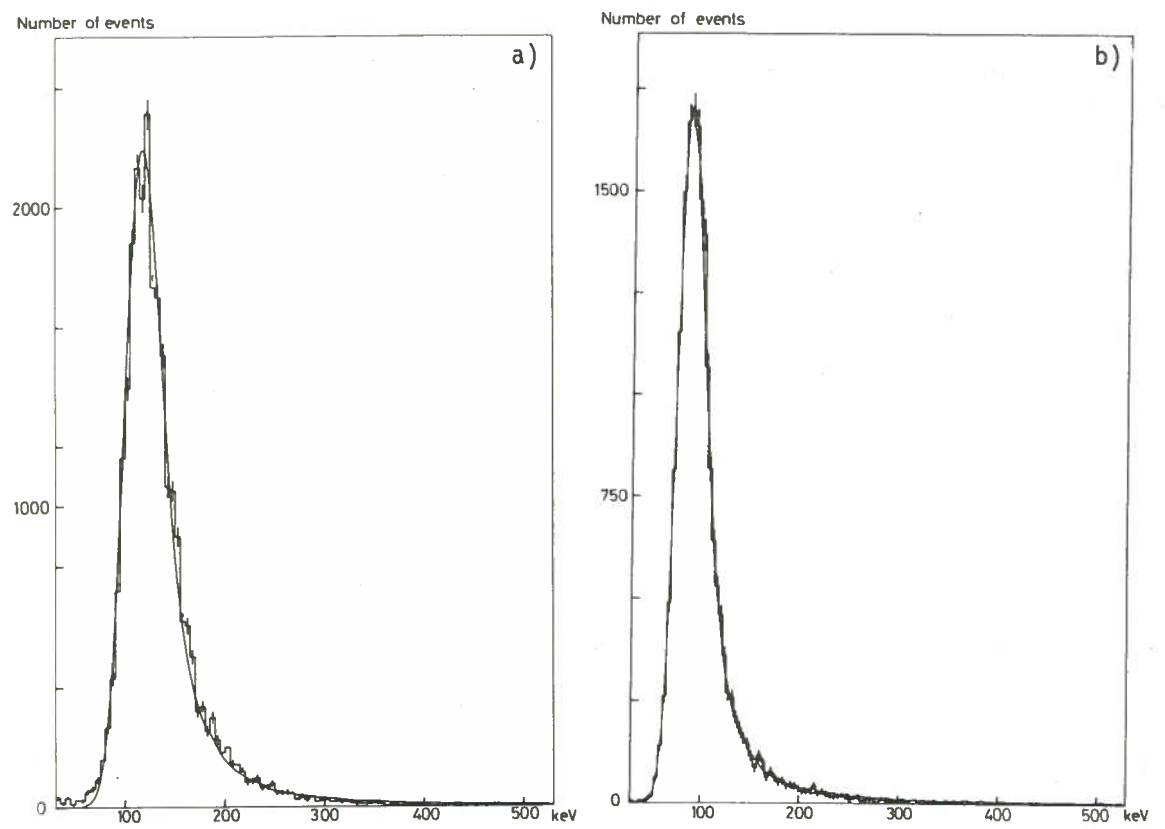

FIG. 7 - Single hit energy-loss distribution. The continuos lines represent the fitted distributions (Landau distribution convolved by a gaussian function, eq. (4)): a) 400 μm thick and 200 μm strip pitch surface-barrier detector, b) 300 μm thick and 200 μm strip pitch ion-implanted detector.

3. 3. - Magnetic field effect

The charge collection in silicon microstrip detector has been investigated by using a 280 μm thick and 20 μm pitch strips device[25] with individual readout. The strips were oriented horizontally, parallel to magnetic field and perpendicular to the incoming 200 GeV/c beam. The effects on both hole and electron collection have been studied.

Without magnetic field the charge distribution is symmetric with a FWHM of 6 μm (for holes) at 120 V (Fig. 8a) and decreasing to 4.5 μm at 200 V. The distribution agrees with the expectation from charge diffusion in silicon.

The magnetic field causes the charges to drift at an angle Θ_L with respect to the direction of the electric field. The value of the drift angle is expected to be

$$tg(\Theta_L) = \mu_H \, H \, 10^{-4}$$

where μ_H[26] is the Hall mobility and H is the magnetic field in T.

A systematic shift of the measured coordinate of about 10 μm (for holes) and an increase in the width of the collected charge distribution to about 12 μm (Figs. 8b and 8c) was observed by applying a magnetic field of 1.68 T. The mean expected shift of 7.3 μm (37.9 μm) for holes (electrons) was in agreement with the measured one[25].

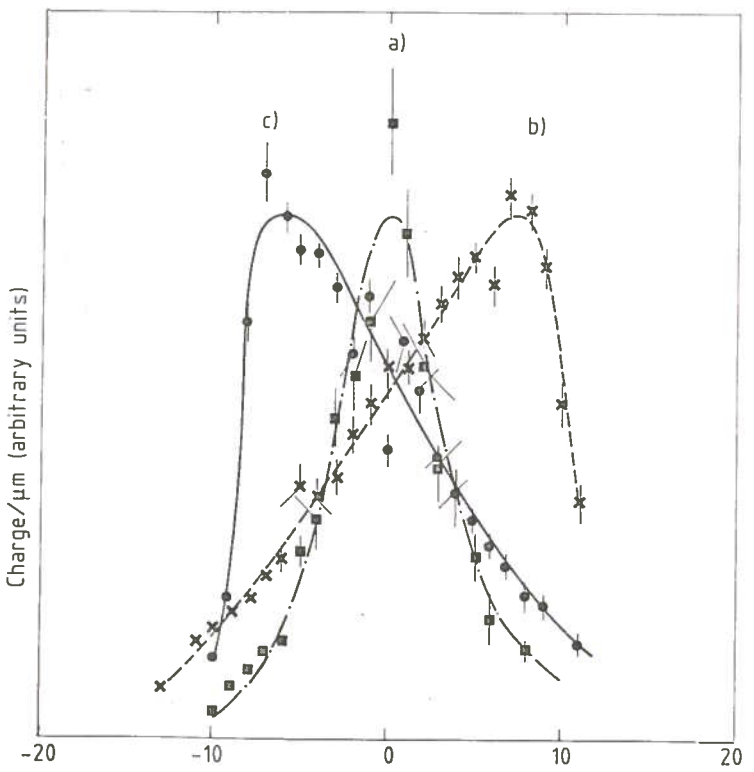

FIG. 8 - Collected charge (holes) distribution[25]: a) no magnetic field applied, b) with a magnetic field of 1.68 T, c) with a magnetic field of - 1.68 T. The continuous lines are the fitted charge distributions.

4. - HIGH-ENERGY PHYSICS APPLICATIONS OF SILICON DETECTORS

Important technological developments regarding silicon detectros have started after the experimental evidence of the short-lived $D\bar{D}$ particle production. They have allowed the use of highly compact multilayer targets. Sets of microstrip devices are now currently located downstream the target in charm and beauty search experiments.

They look atractive for colliding beam machine experiments. Therefore large scale integration (LSI) preamplifier chips and large area silicon detectors for calori-

metry applications are currently investigated.

4. 1. - Fixed target experiments

4. 1. 1. - NA1-experiment

A measurement of D^+D^- lifetime has been proposed (and performed) by the NA1 photoproduction experiment at CERN-SPS. The target was an active miltilayer silicon detector. Incoming photons whose energies were greater than about 100 GeV produced the $D\overline{D}$ system on silicon coherently. At these energies, the two particles had the mean decay path of a few mm in the laboratory. Thus the target consisting of 40 detectors (300 μm thick and 150 μm spaced) could either select coherent reactions or detect a multiplicity step at the decay position[27] of the short-lived particles[28].

A total amount of 86 D^+D^- candidates[29] were selected asking that: i) $M_1 + M_2$ (M_i is the reconstructed mass of the charmed particle) is between 3.66 and 3.90 GeV/c^2, ii) a coherent signal is followed by a multiplicity level of 2 and one or two steps (Fig. 9).

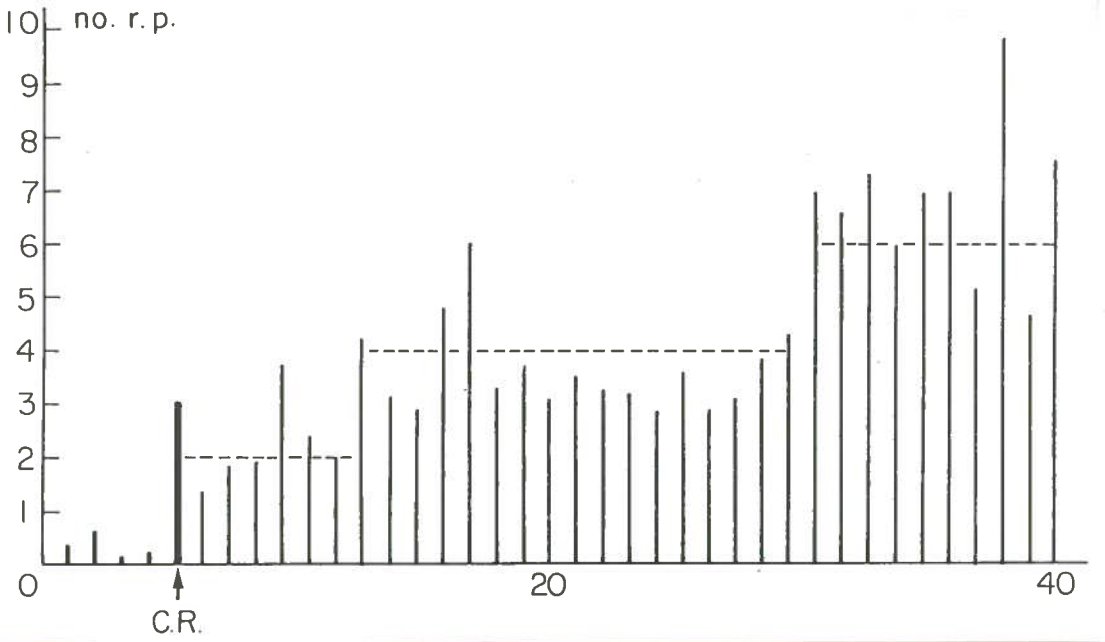

FIG. 9 - Energy-loss (in number of relativistic particles) for a candidate D^+D^- event photoproduced coherently on Si, as sensed by the NA1 active target[28]. Each detector is 300 μm thick and 150 μm is the spacing (along the beam direction) between the detectors, C. R. indicates the signal corresponding to a recoiling Si nucleus, its energy-loss is consistent with a coherent reaction.

Unfortunately, an unambiguous identification of the final state could not be obtained because no tracking microstrip device was associated to the target. It was assumed

$$\gamma_{D^+} = \gamma_{D^-} = E \text{ (energy of the incoming photon)}/2m_D$$

where m_D is the mass of the $D^{\pm}$ meson.

The time distribution of the decays is shown in Fig. 10[28]. The background (mainly γ-ray conversions) was estimated to be about 10%. Steps due to D^o decays were evaluated to be about 20%. An overall fit to the data taking into account these two contributions gave

$$D^{\pm} = 9.5^{+3.1}_{-1.9} \times 10^{-13} \text{ s}.$$

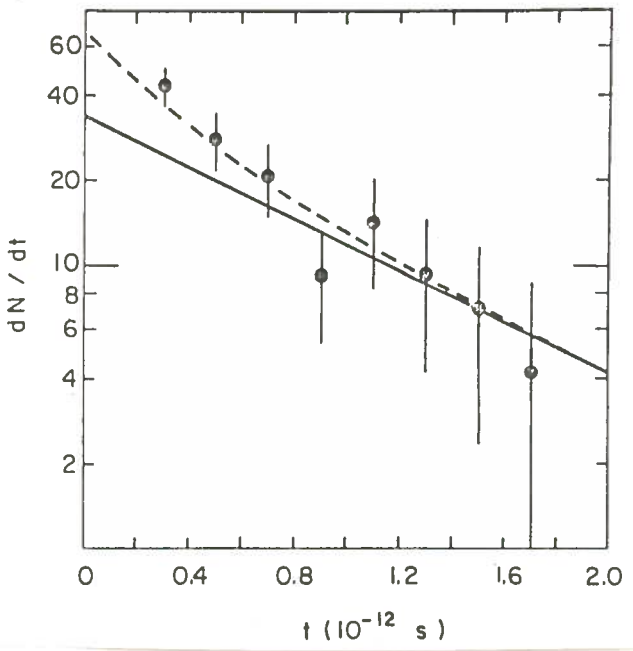

FIG. 10 - Time distribution of identified charmed particle decays. The continuous line gives the $D^{\pm}$ contribution and the dashed line is the overall fit to the data, taking into account a D^o contamination of the order of 20%[28].

4.1.2. - NA11-experiment

For the heavy flavour program of the NA11 experiment[31] at the CERN-SPS, the silicon high-resolution vertex detector is the major instrument.

The beam telescope consists of 6 planes of microstrip detectors (Fig. 11a). The first 4 have horizontal strips of 50 μm pitch arranged in pairs staggered by 25 μm. The last 2 have strips aligned $\pm 14^o$ to the horizontal and of 20 μm pitch. The impact position of the incoming 200 GeV/c π^- particle is measured with a precision of 5 m vertically and 20 μm horizontally. A strong focusing mode provides a beam full width of 250 μm vertically and 15 mm horizontally.

The active target consists of 10 planes of silicon counters 280 μm thick and spaced at 500 μm along the beam direction (Fig. 11b). They have horizontal strip of 20 μm pitch and 26 mm length. Two more Si-detectors with 400 μm pitch strips are located 20 mm downstream. The output pulses from the associated shaping amplifiers are digitized within 10 μs. The information is used by a microprocessor to provide the trigger. The aim is to measure the primary and secondary multiplicities in a narrow forward cone of about 7^o. A charm candidate is accepted if there is a multiplicity change of four.

The vertex telescope (Fig. 11a) consists of 6 silicon strip counters of 280 μm thickness and 24×36 mm^2 sensitive area. They are capacitive charge division detectors (sect. 3.2) and measure one projection with 5 μm resolution. The 6 planes are arranged in two views of $\pm 14^o$ inclination to the horizontal. They allow: i) a precise reconstruction of both the primary and secondary vertices, ii) to reduce considerably the combinatorial background.

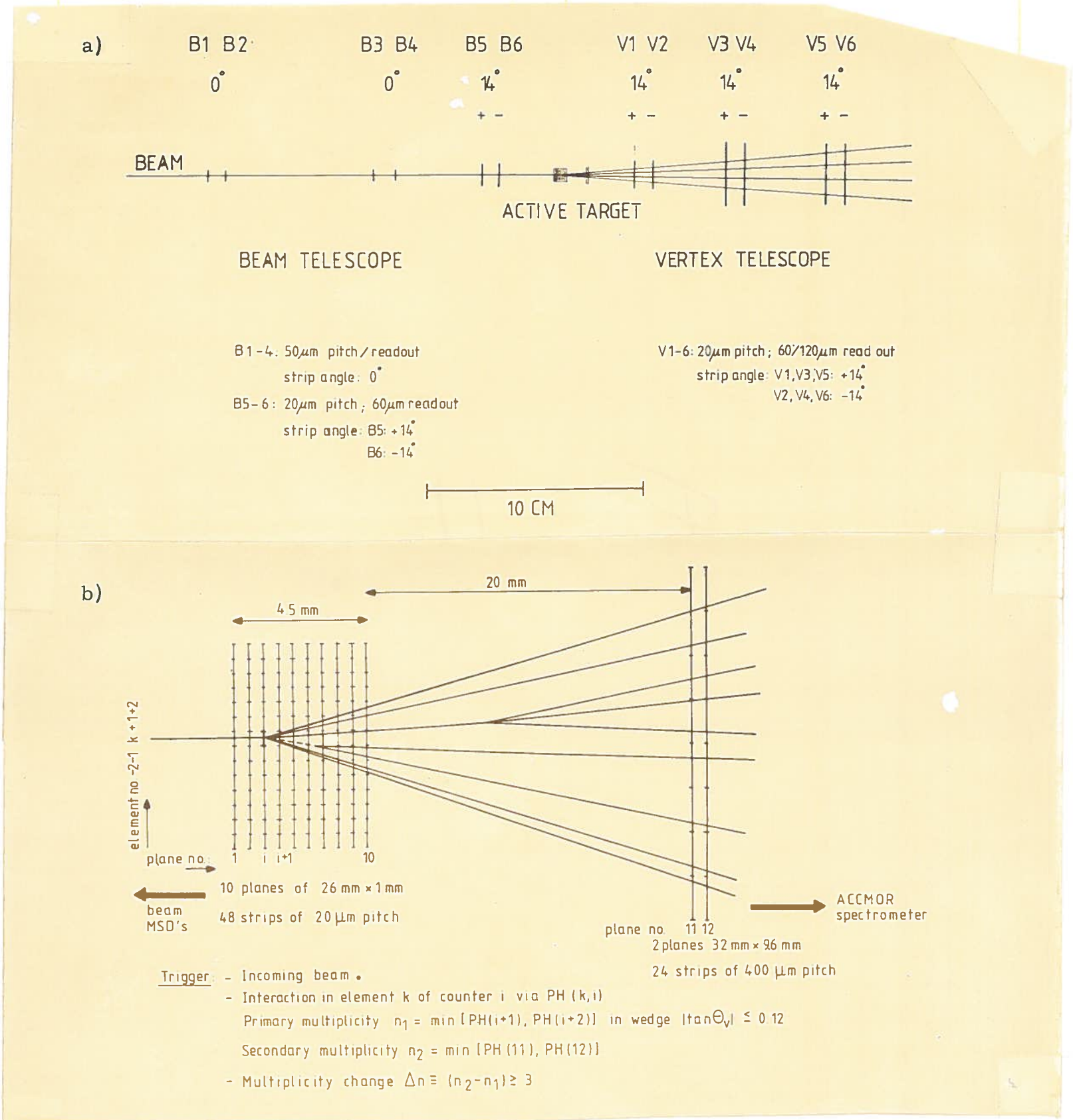

FIG. 11 - a) Lay-out of the NA11 vertex telescope. The B_1-B_4 silicon detectors have horizontal strips of 50 μm pitch. The B_5 and B_6 silicon detectors have strip with 20 μm pitch and aligned $\pm 14^o$ to the horizontal. The V_1-V_6 devices are capacitive charge division detectors. Their resolution is 5 μm. They have strips inclined $\pm 14^o$ to the horizontal. b) Lay-out of the NA11 active target: 10 planes of silicon detectors with 20 μm pitch strips and spaced at 500 μm of distance along the beam. Two microstrip detectors with 400 μm pitch strips are located 20 mm downstream.

4. 1. 3. - NA14-experiment

This experiment[32] uses the high intensity tagged photon beam at CERN-SPS. The primary electron beam intensity is about 2×10^8 e^-/burst with a momentum of 175 GeV/c.

The target is a multilayer silicon detector (Fig. 12). There are 30 planes, each 300 μm thick and spaced by 200 μm. Each plane has an active area of 20 cm^2 and is splitted in 24 vertical strips, whose width is 2 mm. A 31st detector with horizontal strips is added downstream. A set of 4 microstrip doublets is located after the target (Fig. 13). Each doublet is spaced by 1.5 cm and the first one is 1.5 cm from the multi layer silicon detector. The first three doublets have the strips oriented vertically and

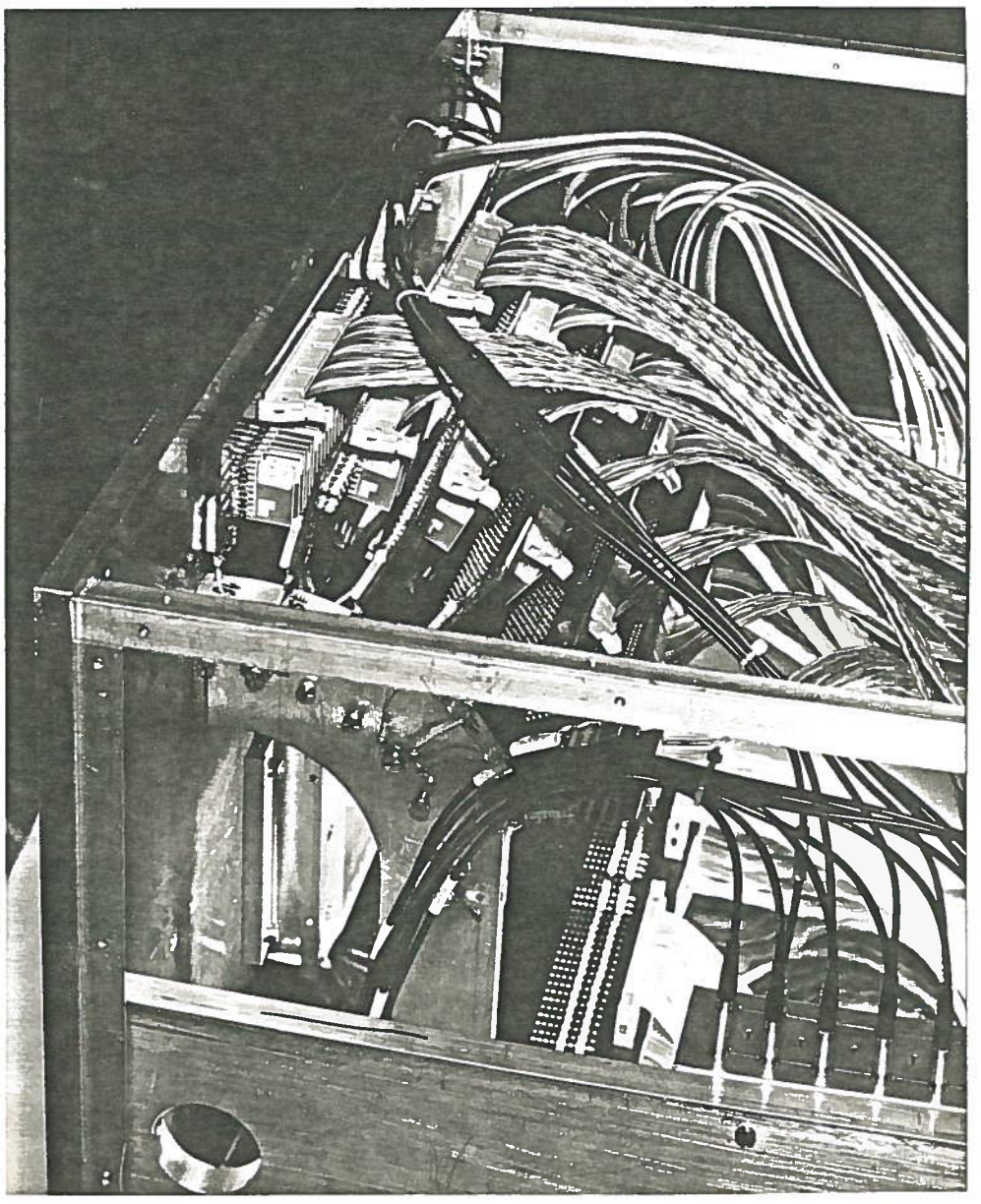

FIG. 12 - Side view of the NA14 multilayer silicon target. Each layer, 300 μm thick, is splitted in 24 detectors whose width is 2 mm. The strips are vertical. The beam is coming from the right.

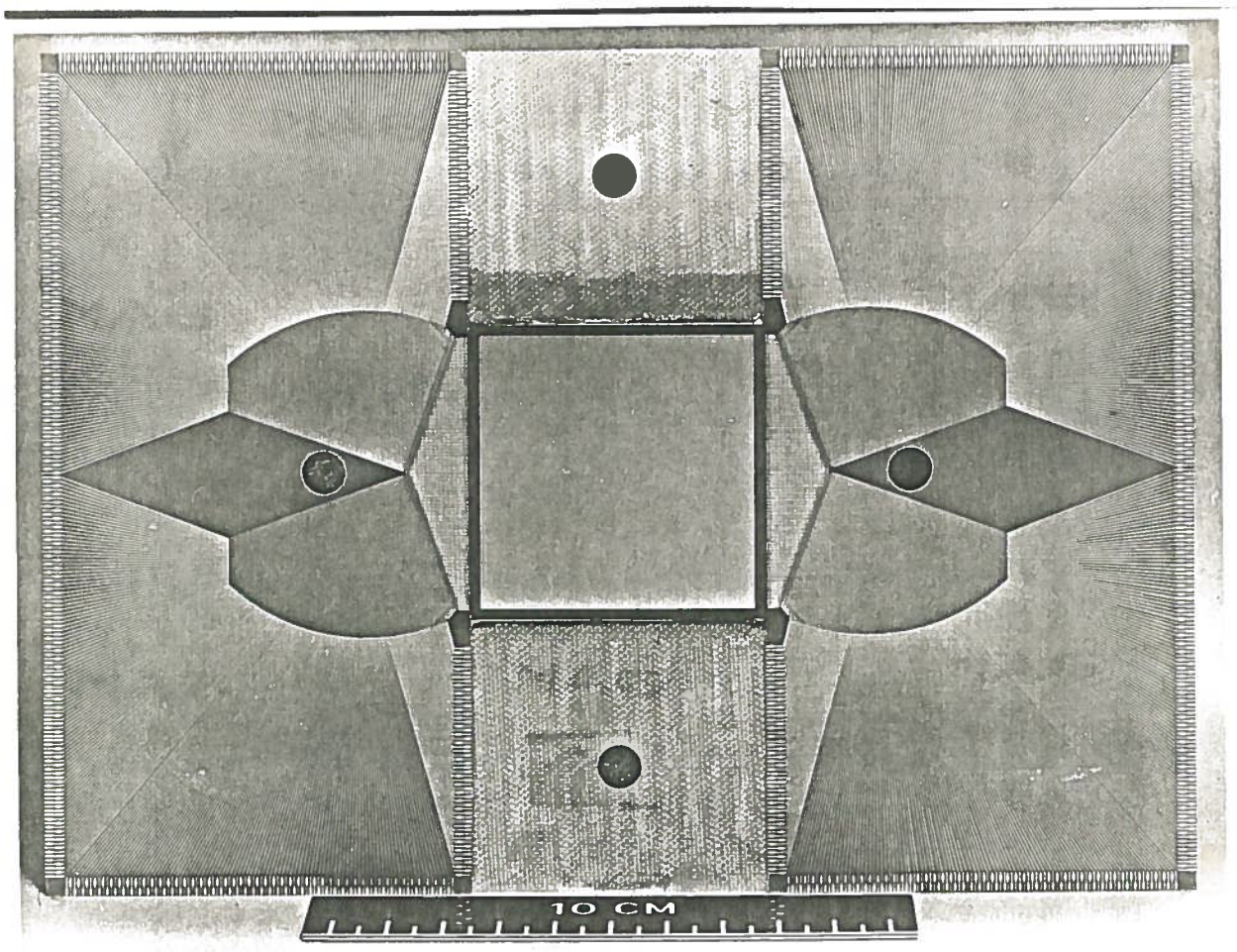

FIG. 13 - Microstrip detector with active area of 5×5 cm^2. The strip pitch is 50 μm. Each strip is connected to fast electronics with $\approx$15 ns rise- and $\approx$ 25 ns fall-time of the signal.

horizontally. The fourth one has the strips at $\pm 15^{o}$ with the horizontal. Each detector has an active area of 5×5 cm^2 and the strip pitch of 50 μm. Fast electronics ($\approx$50 ns of signal base-time) is associated to both the multilayer target and the microstrip detectors. This way the active vertex can stand the very high counting rate due to the electromagnetic background. The counting rate in each strip of the last target layer is $\approx 5 \times 10^5$ counts/burst.

The experiment will start the data taking on heavy flavour photoproduction during 1984. The informations from the active vertex will be used off-line: i) for selecting the charm candidate, ii) for localizing the decay vertices, and iii) for properly associating the tracks to their vertices. The filtering procedure flags a charmed meson candidate when off set tracks[33] are obtained from the reconstruction in the microstrip detectors and one or two steps in multiplicity are detected in the multilayer target. A sample of about 50-200 fully reconstructed charmed events per decay channel is expected.

The multilayer target has already been tested. A tungsten dump with a length of 85 cm was located downstream the device. The trigger was formed by requiring that an incident photon interacts in the target and one or two muons were emerging from the dump. This way an enriched charm sample was expected. The active target worked satisfactorally, except for four unbiased layers. In Fig. 14 an event with a multiplicity step is shown. The interaction layer has sensed an energy-loss compatible with that expected for the coherent recoil of a silicon nucleus. The following layers detect two and the others four relativistic particles. On the left side the height corresponding to the most probable energy-loss of 10 relativistic particles is given. The spurious hits around the interaction are due to the electromagnetic background.

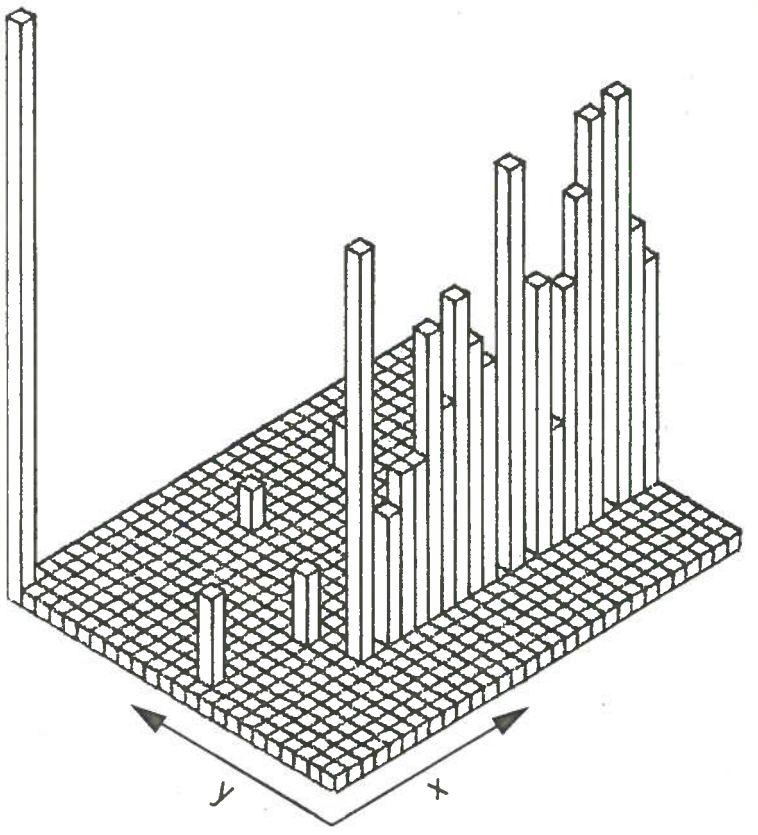

FIG. 14 - Multiplicity step sensed by the NA14 multilayer target. The y-axis is 4 cm long and the x-axis is 1.5 cm long. At left, the energy-loss corresponding to 10 relativistic particles is given.

4.1.4. - Hybrid experiments

Some fixed target experiments (Table II) are planning to employ a hybrid technique, namely an emulsion target followed by microstrip detectors (exp. WA71 at CERN-SPS[34], exp. WA75 at CERN-SPS[35], exp. E653 at Fermilab[36]). The silicon counters provide a resolution of $\approx 10\ \mu m$ in the plane of the emulsion sheets and $\approx 200\ \mu m$ along the beam direction. They locate the interaction vertex and off set tracks and allow a substantial improvement in the identification of events in the emulsion. Therefore it is possible to reduce the number of events to be scanned. The charmed or beauty particle candidate is decided by observing the decay vertex in the emulsion. Usually a beam hodoscope consisting of silicon detectors gives the impact coordinates on the target.

In the WA 71 experiment at CERN-SPS, two multilayer silicon detectors are placed in between the target and the set of microstrip devices. An on-line pulse-height analysis is performed. The multiplicity of one event is measured at two distances, i.e. at 10 mm, from the target. The event is triggered if a step in multiplicity greater than or

equal to two is detected.

TABLE II - Hybrid experiments employing silicon detectors for hadroproduction of heavy flavours.

Approved experiment	Associated microstrip detectors	Silicon detectors in trigger
WA 75	7 planes, 300 μm thick, 50 μm pitch and 6 planes for the beam hodoscope	
WA 71	6 planes, 400 μm thick, 50 μm pitch and 2 planes for the beam hodoscope	step in multiplicity detected by 2 silicon multilayer telescopes
E 653	21 planes, 300 μm thick, 40 μm pitch and 2 planes for low angle track measurement	

In general the hybrid technique can achieve a better identification of charmed event candidates. However its main limitation comes from the number of events, which can be actually scanned.

4. 2. - Colliding beam machine experiments

At the very high energy at which an interaction occurs in the current and forthcoming colliding beam machines, silicon detectors can provide a wellsuited high-resolution vertex detector. Thus a separation of the heavy flavour decay vertices from the interaction vertex is achievable. Furthermore it improves the momentum resolution of the central detector. The construction of a large area mosaic of detectors does not seem to have too many difficulties. However the high resolution is thought to be obtained by the individual readout of very fine pitch ($\approx 25\ \mu$m) strips. In the sect. 4.2.1, a project in which a "microplex" readout chip is under investigation is described.

The silicon detectors can find application in calorimetry as active sampling layer. They operate in magnetic enviroments, where there are geometric constraints or in vacuum. Large-size inexpensive devices are manufactured by using low-resistivity ($\approx 1500\ \Omega$ cm) material. Although the counter works as undepleted device, in calorimetry a sensitive volume of about 50% of the physical one is sufficient due to the large number of traversing particles.

4. 2. 1. - Microvertex and large-scale integration

The proposed microvertex for DELPHI experiment at LEP[3] consists of three concentric cylinders of silicon wafers. The radius of the inner cylinder is $\approx$ 8-9 cm and is close to the vacuum pipe. An assembly of 30 unit "cells", in average, builds up a cylinder (Fig. 15). A cell consists of an open quartz frame, onto which are guided: i) 7 detectors, each with active area of 6 x 2.5 cm^2 and a thickness of 300 μm, ii) 10 readout chips, each with an area of 0.4 x 0.6 cm^2 and a thickness of 380 μm, and iii) 10 (or less) driver chips, each with an area of 0.4 x 0.5 cm^2 and a thickness of 380 μm. The microstrip detectors are interconnected by wire bonding. The strip pitch is 25 μm.

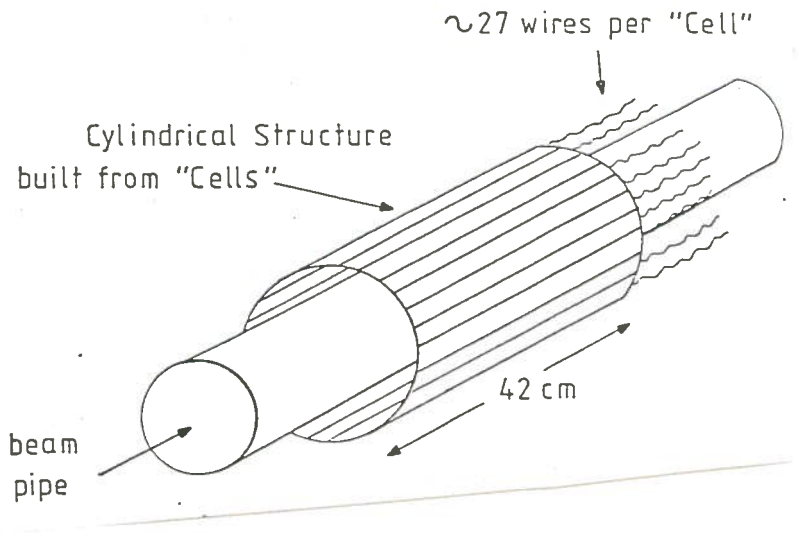

FIG. 15 - Lay-out of one silicon cylinder of the proposed microvertex for DELPHI experiment at LEP.

The "microplex" readout is still under computer design. The technology is standard, but the design is unusual, combining large-scale integration (LSI) with low noise. It is expected to have an excellent noise performance, i. e. the gaussian noise distribution has a standard deviation $\sigma \approx 4$ keV. The rise-time of the amplifier signal is $\approx$ 10 ns. Every chip has 128 channels.

4. 2. 2. - Silicon detectors and calorimetry

Silicon detectors can be used in sandwich calorimeters as active sampling layers. Due to the small amount of energy necessary to create an e-h pair ($\approx$ 3.6 eV), they allow to build up very compact calorimeters. They may work at room temperature and their electronics is easily accomodated nearby.

The large-size active areas are achieved by employing inexpensive low resistivity material[4], cut to a standard thickness of $\approx$ 300 μm. Thus, as mentioned above, the detectors work as undepleted devices. In actual practice the sensitive region is the charge-depletion layer plus an additional region, the thickness of which is a fraction of a carrier diffusion length

$$L = \sqrt{(D\tau)}$$

where D is the diffusion coefficient[37] of the minority carriers, i. e. the holes in an n-type bulk silicon, and τ is the minority carrier lifetime. In the case of relativistic particles traversing an undepleted detector, only minority carriers created by the energy lost in a region of $\approx 6\ \mu m$ may migrate from the field-free region into the space--charge region. For an n-type silicon, the depleted space-charge region is

$$d = 0.53 \sqrt{(\varrho V)} \quad (\mu m)$$

where ϱ is the resistivity in Ωcm and V is the applied reverse bias. As an example, a detector made using a 1500 Ωcm wafer, has a depleted layer of $\approx 160\ \mu m$ at 60 V of reverse bias.

To prove the feasibility of using undepleted detectors, a test was performed on an ion-implanted detector of 7 kΩ cm resistivity, 300 μm thickness and $1 \times 1\ cm^2$ active area, using a 30 GeV/c pion beam at CERN-SPS[4]. At any applied voltage lower than that required for full depletion, the resulting energy-straggling spectrum sensed by the detector was in agreement with the modified energy-loss distribution (eq. (4)) of a relativistic particle traversing a silicon absorber of thickness equal to the current depleted layer. In Fig. 16, the energy-loss spectra obtained at 55 V and 10 V are shown. The corresponding depleted layers were 300 μm (fully depletion) and $\approx 200\ \mu m$ respectively. The continuous lines are the fits to eq. (4) including the gaussian noise contribution.

In a silicon sandwich calorimeter, the energy resolution is only limited by the sampling fluctuations owing to the silicon density. Thus using tungsten a showering material, the expected energy resolution[38] for a fully depleted contained shower and one sampling per radiation length is $\approx 9.2\%/\sqrt{E}$. The total energy is contained in a cylinder having a radius of ≈ 1.8 cm. About 26 radiation lengths are necessary to the fully longitudinal shower containement for incoming electron energies up to 50 GeV. The physical length of this sandwich calorimeter is about 10 cm.

At present silicon/lead or silicon/tungsten calorimeters are likely to be built as LEP luminosity monitor and forward electron tagger at HERA machine. In both cases a set of microstrip detectors are located upstream in order to track the incoming electron. They are supposed to be placed around the beam pipe.

A prototype of the silicon/tungsten calorimeter will be tested at the X7 electron beam at CERN-SPS, starting from summer 1983. It consists of 15 tungsten layers, each one of two radiation lengths and interspaced by a $5 \times 5\ cm^2$ low resistivity (≈ 1500 Ωcm) silicon detector as active sampling layer.

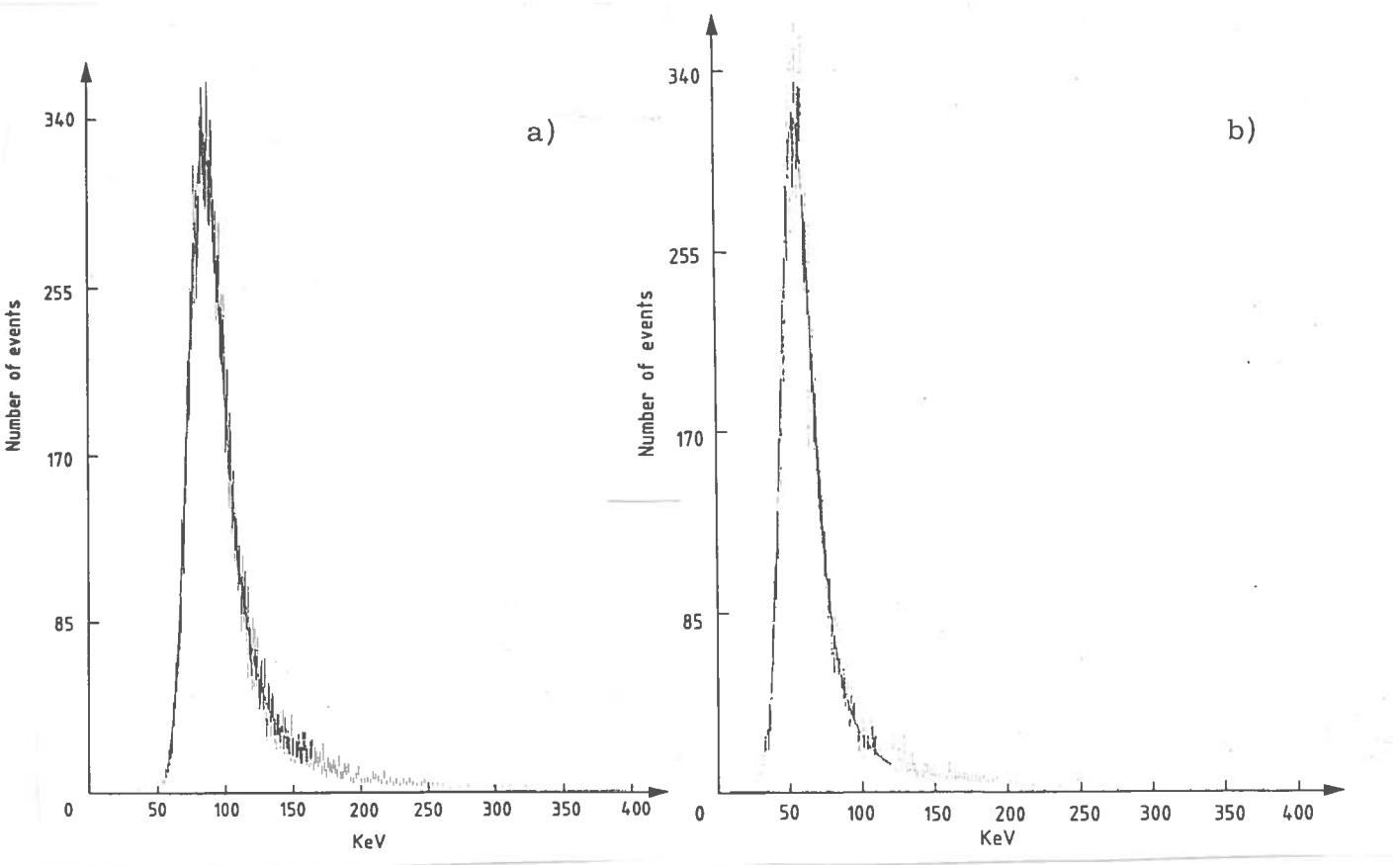

FIG. 16 - a) Energy-loss of a relativistic pion traversing a 300 μm Si-detector. The applied reverse bias is 55 V corresponding to that necessary for full depletion. The continuous curve is the best fit to a Landau distribution convolved by a Gaussian. The most probable energy-loss is 83.8 ± 4.2 keV. The FWHM of the Landau distribution is 23.1 ± 1.2 keV. The FWHM of the Gaussian (with the noise contribution subtracted) is 13.2 ± 0.7 keV. b) Energy-loss of a relativistic pion traversing a 300 μm Si-detector. The applied reverse bias is 10 V. The detector is operating as an undepleted detector. The continuous curve is the best fit to a Landau distribution convolved by a Gaussian. The most probable energy-loss is 53.2 ± 2.7 keV. The FWHM of the Landau distribution is 16.7 ± 0.8 keV. The FWHM of the Gaussian (with the noise contribution subtracted) is $11.4 \pm \pm 0.6$ keV.

5. - CONCLUSION

The silicon detectors have been employed in high-energy physics since 15 years. However spectacular advances occurred in the past three years.

Complex detector configurations are now possible for heavy flavour fixed target experiments. They have microstrip detectors downstream the target, which is a multilayer silicon or emulsion sheets. The secondary vertices can be located with precision of a few hundred microns by analysing the energy-loss data, when a silicon target is used.

Large-area detectors are proposed as microvertex in colliding beam machine experiments. They are well-suited as high resolution inner detector in order to untangle

decay vertices of produced heavy flavours and to improve the momentum resolution of the central detector. A new deal of technological development is currently oriented to produce large scale integration preamplifier chips.

The silicon detectors find application in calorimetry as dense active sampling layer. The calorimeter energy resolution is only limited by the sampling fluctuations. Large area devices are built by using inexpensive low resistivity detectors, which operate as undepleted counters. Their sensitive region is given by both the charge depletion layer and a few microns in the field-free region.

ACKNOWLEDGMENTS

The author is particularly indebeted to Prof. A. Seidman for his suggestions, for reading and correcting the manuscript. Useful discussions with P. Borgeaud, I. Siotis, D. Treille and D. Websdale are gratefully acknowledged.

REFERENCES AND FOOTNOTES

(1) - P. G. Rancoita and A. Seidman, Silicon detectors in high-energy physics : physics and applications, Riv. Nuovo Cimento 5, n. 7 (1982).

(2) - B. Hyams, W. Koetz, E. Belau, R. Klanner, G. Lutz, E. Neugebauer, A. Wylie and J. Kemmer, Nuclear Instr. and Meth. 205, 99 (1983).

(3) - M. Bosman, B. Hyams, P. Weilhamer and A. Zalewska, DELPHI group note no. 1 (1983).

(4) - G. Barbiellini and P. G. Rancoita, A luminosity monitor for LEP using electro magnetic calorimeters : the silicon/lead sandwich, CERN-EP Internal Report 83-01 (1983).

(5) - J. Kemmer, Nuclear Instr. and Meth. 169, 499 (1980).

(6) - E. Heijne, Radiation damage : experience with silicon detectors in high-energy beams at CERN, CERN EF-BEAM 81-6 (1981).

(7) - P. Borgeaud, G. McEwen, P. G. Rancoita and A. Seidman, Nuclear Instr. and Meth. 211, 363 (1982).

(8) - L. Landau, J. of Phys. (USSR) 8, 201 (1944).

(9) - W. Boersch-Supan, J. Res. Natl. Bur. Stand. 65B, 245 (1961).

(10) - P. V. Vavilov, Soviet Phys. -JETP 5, 749 (1957).

(11) - D. W. Aitken, W. L. Lakin and H. R. Zulliger, Phys. Rev. 179, 393 (1968).

(12) - S. Hancock, F. James, J. Movchet, P. G. Rancoita and L. Van Rossum, Phys. Rev. A28, 615 (1983).

(13) - U. Fano, Ann. Rev. Nucl. Science 13, 1 (1963).

(14) - H. Bichsel and P. Saxon, Phys. Rev. A11, 1286 (1975).

(15) - H. Bichsel, Phys. Rev. B1, 2844 (1970).

(16) - P. Shulek, B. M. Golovin, L. A. Kulyukina, S. V. Medved' and P. Pavlovich, Soviet J. Nuclear Phys. 4, 400 (1967).

(17) - R. M. Sternheimer, Phys. Rev. 145, 247 (1966).

(18) - H. Bichsel, private communication (1981).

(19) - H. Bichsel and S. Yu, IEEE Trans. Nuclear Sci. NS-19, vol. 6 172 (1972). In this paper the quantity D/E_m ($D = \delta_2/2\xi$) has been computed by Bichsel for an incoming proton with kinetic energies between 0.1 and 10 GeV.

(20) - H. Esbensen, O. Fich, J. A. Golovchenko, S. Madsen, H. Nielsen, H. E. Schitt, E. Uggerhj, C. Vraast-Thomsen, G. Charpak, S. Majewski, G. Odyniec, G. Petersen, F. Sauli, J. P. Ponpon and P. Siffert, Phys. Rev. B18, 1039 (1978).

(21) - R. M. Sternheimer, Phys. Rev. B3, 3681 (1971).

(22) - S. Hancock, F. James, J. Movchet, P. G. Rancoita and L. Van Rossum, Energy--loss distributions for single and several particles in a thin silicon absorber, CERN-EP/83-138 (1983), and to appear in Nuclear Instr. and Meth.

(23) - P. Bonamy, P. Borgeaud, J. Movchet and P. G. Rancoita, Performance of surface barrier and ion-implantation silicon detectors, CERN EP-Internal Report 81-06 (1981), and Proc. of the Semiconductor Detector Workshop, Fermilab 15-16 Oct. 1981, Ed. by T. Ferbel (1982), p. 257.

(24) - A single hit event occurs when a single strip detects a signal greater than $3\sigma_{noise}$ (σ_{noise} is the standard deviation of the noise gaussian distribution). A double hit event occurs when two neighbouring detect signals greater than $3\sigma_{noise}$.

(25) - E. Belau, R. Klanner, G. Lutz, E. Neugebauer, H. J. Seebrunner, A. Wylie, T. Bohringer, L. Hubbeling, P. Weilhammer, J. Kemmer, U. Koetz and M. Riebesell, Nuclear Instr. and Meth. 214, 253 (1983).

(26) - Typical values of μ_H are 310 cm^2/Vs for holes and 1650 cm^2/Vs for electrons.

(27) - The reconstruction procedure is explained in sect. 2.

(28) - E. Albini, S. R. Amendolia, R. Baldini Celio, G. Batignani, F. Bedeschi, G. Bellini, E. Bertolucci, B. Bettoni, G. Bologna, L. Bosisio, C. Bradaschia, M. Budinich, F. Celani, A. Codino, M. Dell'Orso, B. D'Ettorre Piazzoli, M. De Vincenzi, F. L. Fabbri, F. Fidecaro, L. Foa', E. Focardi, A. Giazotto, M. A. Giorgi, P. Laurelli, M. Leopold, F. Liello, P. F. Manfredi, G. Mannocchi, P. S. Marrocchesi, A. Menzione, E. Meroni, L. Moroni, C. Palazzi Cerrina, L. Petrillo. M. L. Piazzi, P. Picchi, M. Quaglia, F. Ragusa, P. G. Rancoita, L. Ristori, G. Rivellini, L. Rolandi, S. Sala, L. Satta, A. Scribano, M. Severi, P. Spillantini, A. Stefanini, R. Stanga, M. L. Vincelli, A. Zallo and I. O. Zielinski, Electronic measuremen of the lifetime of D^{+-} mesons, CERN-EP/82-12 (1982), and Phys. Letters 110B, 339 (1982).

(29) - A detailed discussion of the data analysis is given in refs. (28) and (30).

(30) - G. Bellini, L. Foa' and M. Giorgi, Phys. Report 83, 9 (1982).

(31) - ABCCMR (Amsterdam-Bristol-CERN-Cracow-Munich-Rutherford) collaboration, Investigation of charm production in hadronic interactions using high-resolution silicon detectors, CERN/SPS/82-57 SPSC/P180 (1982).

(32) - ACLOPPSSSW (Athens-CERN-London(I. C.)-Orsay-Palaiseau(Ec. Pol.) - Paris (Col. de France)-Saclay-Southampton-Strasbourg-Warsaw) collaboration, A program of heavy flavour photoproduction, CERN/SPSC/82-73 SPSC/P109 Add. 2 (1982).

(33) - An off set track is at more than about 80 μm from the interaction vertex. The track is reconstructed by using the data from the microstrip detectors.

(34) - CGMMPR (CERN-Genoa-Milan-Moscow-Paris(LPNHE)-Rome) collaboration, An experiment for studying beauty production and lifetime in the upgraded Ω' spectrometer, CERN/SPSC/81-18 SPSC/P159 (1981).

(35) - BBCDKKLNNRTUY (Bari-Brussels-CERN-U. C. Dublin-Kariya-Kobe-U. C. London-Nagoya Univ. -Nagoya Inst. -Roma-Torino-Utsunomiya-Yokohama) collaboration, An experiment to observe directly beauty particles selected by muonic decay in emulsion to estimate their lifetimes, CERN/SPSC/81-69 SPSC/P166 (1981).

(36) - N. M. Reay, A proposal to measure charm and B via hadronic production in hybrid emulsion spectrometer, Fermilab (1981).

(37) - The diffusion coefficient is

$$D = \mu kT/e$$

where k is the Boltzmann constant, T is the absolute temperature, e is the electron charge and μ is the carrier mobility.

(38) - U. Amaldi, Physica Scripta 23, 408 (1981).